ChemComm
Chemical Communications

Accepted Manuscript

This article can be cited before page numbers have been issued, to do this please use: H. Dokken, T. Rajeshkumar, C. C. Almquist, W. Zhou, C. Maichle-Moessmer, A. Harrison, R. Anwander, L. Maron and W. Piers, *Chem. Commun.*, 2026, DOI: 10.1039/D6CC02936A.

ROYAL SOCIETY OF CHEMISTRY

rsc.li/chemcomm

ChemComm

View Article Online
DOI: 10.1039/D6CC02936A

COMMUNICATION

Coordination-induced bond weakening of multiple C-H bonds in a molybdenum methyl complex leading to a bridging ethylenediyl by C-C bond formation through bimolecular coupling of a terminal methylidyne

Received 00th January 20xx,
Accepted 00th January 20xx

DOI: 10.1039/x0xx00000x

Hannah J. Dokken,[a] Thayalan Rajeshkumar,[b] C. Christopher Almquist,[a] Wen Zhou,[a] Cäcillia Maichle-Mössmer,[c] Alexander Harrison,[a] Reiner Anwander,[c] Laurent Maron*[b] and Warren E. Piers*[a]

Activation of C-H bonds in a molybdenum methyl complex by coordination-induced bond weakening was demonstrated by abstracting three hydrogen atoms with an aryl oxyl reagent. The final product is a Mo=C=C=Mo complex arising from coupling of a molybdenum methylidyne intermediate and subsequent removal of the final hydrogen atom equivalent.

Coordination-induced bond weakening (CIBW)[1] is an effective means of activating the strong E-H bonds of protic molecules like water (O-H = 110 kcal mol^{-1})[2] or ammonia (N-H = 99 kcal mol^{-1}).[3] The extent to which E-H bond dissociation free energies (BDFEs) are lowered upon coordination of EH_n to a metal is dependent on two physical properties, the oxidation potential of a given M^n/M^{n+1} redox couple (E^0_{ox}) and the pK_a of coordinated EH_n in the oxidized species, as governed by the Bordwell equation,[4] Fig. 1a. In most instances, these two properties "thermodynamically compensate"[5, 6] for each other, since higher oxidation states lead to lower pK_as while more positive values for E^0 diminish the contribution of this term to CIBW, leading to minimal changes in E-H bond dissociation free energy (BDFE) given on the diagonal of a "square scheme".[3] However, with judicious choice of metal (reducing) and ligand (electron rich), these factors can be influenced such that E^0 becomes dominant and significant E-H BDFE weakening for coordinated H_2O or NH_3 ligands in comparison to the free molecules is enabled, facilitating abstraction of hydrogen atoms by aryl oxyl reagents ArO•. If CIBW draws the E-H BDFE below ≈ 52 kcal mol^{-1}, spontaneous elimination of H_2 becomes thermodynamically plausible—if a low barrier path is available.[7]

While a variety of low valent metal systems have been shown to engender CIBW in protic substrates,[1] group 6 metals have proven especially effective due to the availability of a range of oxidation states/redox couples at moderate voltages. Bezdek and Chirik have demonstrated that a cationic, octahedral Mo(I) system (**I**, Fig. 1b) significantly weakens the first N-H bond of ammonia[7] and other amine substrates.[8-10] The L_5 ligand environment here dictates that lower oxidation states are required; we postulated that molybdenum complexes of our more electron rich L_3X_2 diborate-based pentadentate ligand

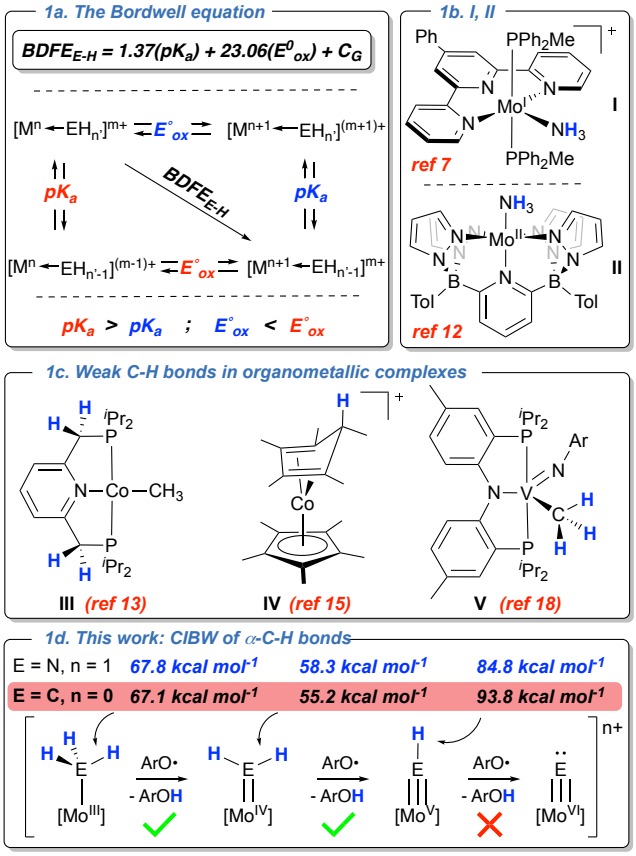

Fig. 1 a) General square scheme for E-H CIBW. b) Mo ammine complexes exhibiting significant CIBW. c) C-H CIBW examples. d) Comparative DFT computed gas phase E-H BDFEs for E = N and E = C on a (B_2Pz_4Py)Mo^{III} platform.

[a] Department of Chemistry, University of Calgary,2500 University Dr. NW, T2N 1N4, Calgary, AB, Canada
[b] LPCNO, INSA, UPS, Université de Toulouse, 135 avenue de Rangueil, F-31077, Toulouse, France
[c] Institut für Anorganische Chemie, Eberhard Karls Universität Tübingen, Auf der Morgenstelle 18, 72076, Tübingen, Germany

View Article Online
DOI: 10.1039/D5CC02976A

system **B_2Pz_4Py**[11] (*e.g.* **II**, Fig. 1b) would allow access to higher oxidation state redox couples and facilitate removal of all three hydrogen atoms from ammonia. This proved to be the case, with significant CIBW observed for multiple H• removal in **II**.[12]

In contrast to coordinated ROH or RNH_2, fewer examples of C-H CIBW in aliphatic ligands have been reported.[1] Pincer ligands with benzylic C-H bonds are staples of ligand cooperativity that involve C-H bond cleavages[13] (Fig. 1c, **III**). Protonation of coordinated Cp ligands,[14] exemplified by decamethylcobaltocene **IV**,[15] lead to weak C-H bonds. Both **III** and **IV** involve remote C-H bonds that are relatively acidic; instances of CIBW of the α-C-H bonds of alkyl, alkylidene or methylidyne ligands is less documented.[16] Mindiola *et al.* have reported the abstraction of H• with ArO• from methyl groups in Ti[17] and V[18] complexes (Fig. 1c, **V**) to prepare rare first row terminal methylidene complexes. Given the efficacy of our platform **II** to weaken the E-H bonds of coordinated H_2O and NH_3 ligands, we hypothesized that alkyl groups might also be susceptible to removal of H•. Predictive BDFE computations (gas phase) by DFT suggested this should be the case (Fig. 1d) and allow for the comparison of CIBW tendencies for O-H,[19] N-H[12] and C-H bonds on the same metal-ligand platform.

In this study, we employ the **B_2Pz_4Py** ligand with *para*-tolyl groups on the borate arms (Fig. 2a). The Mo(III) chloride starting material[12] was treated with H_3CMgCl in THF to afford the deep yellow **$MoCH_3$** methyl derivative in excellent yield. This compound was fully characterized and is spectroscopically typical of octahedral Mo(III) complexes of this ligand framework[12] (see ESI). It has a μ_{eff} of 3.58 μ_B (Evans method), indicative of an S = 3/2 state, and the Mo-C bond is 2.183(4)Å

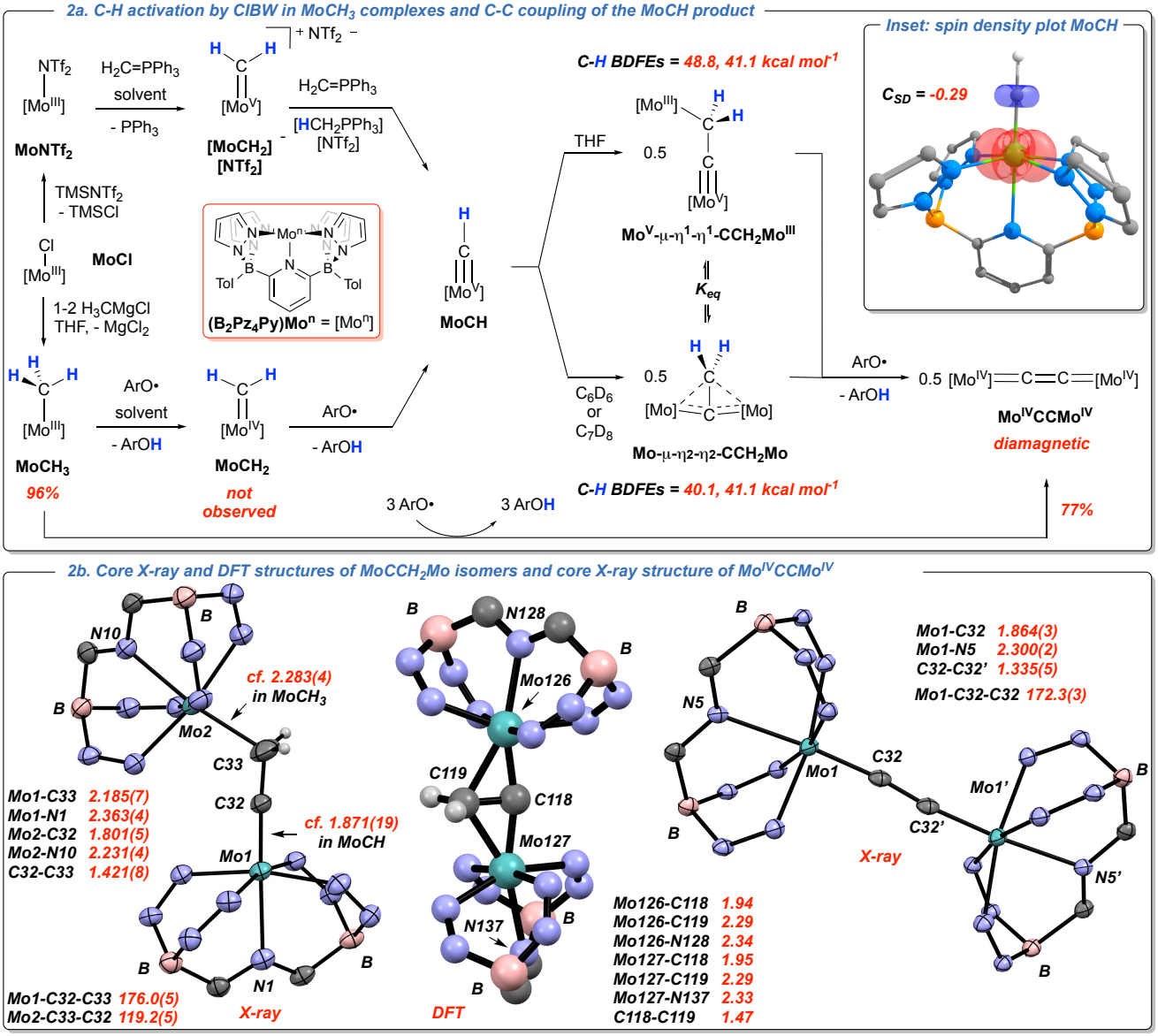

Fig. 2 a) Summary of chemistry discussed herein. b) Core structural features and key metrical parameters of the products of H• abstraction from **$MoCH_3$**. The ORTEP representations of **Mo^V-μ-η¹-η¹-CCH_2Mo^{III}** (left) and **$Mo^{IV}CCMo^{IV}$** (right) have ellipsoids drawn at 50%. The diffraction data for the **Mo-μ-η²-η²-CCH_2Mo** isomer was only sufficient to establish connectivity, so for this isomer the DFT computed (B3PW91 including dispersion) structure of the S = 1 spin state is shown (middle) instead of the ORTEP (for full details of this structure, see ESI). The metrical parameters computed for the S = 1 and S = 0 states of **Mo-μ-η²-η²-CCH_2Mo** are essentially identical.

while the Mo-N_{py} bond *trans* to the methyl group is 2.239(3)Å (Fig. S1). The Mo-N_{py} distances in Mo complexes of **B_2Pz_4Py** ligands can adopt a wide range of ≈ 2.1-2.4Å,[12, 19-21] accommodating ligands of variable *trans* influence in the coordination site not occupied by the pentadentate framework. This metric thus acts as a useful reporter on the characteristics of the ligand in the "active site" of the complexes. A cyclic voltammogram of **$MoCH_3$** reveals an irreversible[22] oxidation wave at 0.08 V vs. Fc^+/Fc^0 in THF (Fig. S2). When oxidized chemically with $[Fc]^+[NTf_2]^-$,[23] ethane is produced (^{1}H NMR, 0.81 ppm in C_7D_8, Fig. S3)[24] along with the previously prepared **$MoNTf_2$**,[12] indicating that the methide group is sufficiently reducing to render the putative **$[MoCH_3]^+[NTf_2]^-$** cation unstable towards Mo-C bond homolysis.

The computed gas phase C-H BDFEs in Fig. 1d suggest that the first two hydrogen atoms of the CH_3 group should be removable with ArO• (Ar = 2,4,6-tri-*tert*-butylphenyl), ArO-H = 77.1 kcal mol^{-1}.[3] This was verified experimentally, although as shown in Fig. 2a, the situation is complicated by the facile coupling of the terminal methylidyne product **MoCH** at rates competitive with H atom abstraction from **$MoCH_3$**. Thus, initial experiments showed that treatment of **$MoCH_3$** with two equivalents of ArO• in C_6D_5Br produced a mixture of compounds, as indicated by multiple tolyl methyl signals in the ^{1}H NMR spectra (Fig. S4-S5), one identified as methylidyne **MoCH** (2.42 ppm), the major component at early reaction times. Starting **$MoCH_3$** was still present (2.31 ppm), but the presumed product of removal of the first H•, methylidene **$MoCH_2$**, was not observed, consistent with its weaker C-H bond strength of 55.2 kcal mol^{-1} relative to **$MoCH_3$** and **MoCH**. Rather, two other tolyl methyl resonances (2.35 and 2.39 ppm) were present in minor amounts, the latter growing in at the expense of the signal for **MoCH** over time, as the methylidyne underwent a bimolecular coupling involving C-C bond formation and hydrogen migration to form the isomers **$Mo^nCCH_2Mo^m$** shown in Fig. 2a (discussed in more detail below). As indicated in Fig. 2a, the C-H bonds in these dinuclear compounds are weakened significantly in comparison to **MoCH**, and are thus subject to further H• abstractions, producing the fully stripped ethylenediyl species **$Mo^{IV}CCMo^{IV}$** (tolyl methyl peak, 2.35 ppm) until the available ArO• is exhausted. This peak intensity remained constant once the ArO• reagent was used up, but the system proceeds cleanly to **$Mo^{IV}CCMo^{IV}$** with addition of further ArO• (1 eq.), or by use of three equivalents of ArO• directly from **$MoCH_3$**; this species is isolated as a sparingly soluble, diamagnetic, purple precipitate in 77% yield.

Samples enriched in methylidyne **MoCH** can be obtained by performing the ArO• abstraction at -32 deg. C in toluene. These solutions were probed by EPR spectroscopy, which initially demonstrated a typical pattern for a d^1 molybdenum complex, suggesting the unpaired electron in **MoCH** is in a metal-based orbital (Fig. S6a). A central resonance with a *g*-value of 1.975 is superimposed onto a six-line hyperfine coupling pattern (A_{Mo} = 146 MHz and A_C = 4.13 MHz) arising from coupling to the ≈ 25% abundant spin 5/2 $^{95/97}$Mo isotopes and to the spin 1/2 ^{13}C isotope of the methylidyne (see Fig. S6b for the simulated spectrum). The spectrum is similar to what was observed for the isoelectronic nitrido complex $(B_2Pz_4Py)Mo^V{\equiv}N$.[20] As seen in Fig. S6a, over time, this resonance diminishes in intensity as **MoCH** undergoes coupling to the EPR silent **$Mo^nCCH_2Mo^m$** products. Crystals grown from these experiments at early reaction times allowed for the structure determination of **MoCH** (Fig. S7; Mo≡C, 1.871(19) Å; Mo-N_{py}, 2.341(12)Å) and assignment of the tolyl methyl resonance for this species at 2.38 ppm in C_7D_8.

DFT computations matched the experimental structure well and showed that significant spin density of -0.29 exists on the methylidyne carbon (inset, Fig. 2a), suggesting the coupling of two **MoCH** has radical character for C-C bond formation. The details of the mechanism leading to the **$Mo^nCCH_2Mo^m$** isomers, which also involves a 1,2-migration of hydrogen, are ill defined at this point, but we note that Templeton *et al.* have observed analogous coupling of related terminal methylidyne complexes $Tp'(CO)_2M{\equiv}CH$ (Tp' = $HB(3,5\text{-}Me_2Me_2C_3HN_2)_3$; M = Mo or W) to M-μ-$\eta^2$-$\eta^2$-$CCH_2M$ products.[25] In the present system, separate synthesis of **MoCH** *via* reaction of the **$MoNTf_2$** starting material with two equivalents of Wittig reagent $H_2C{=}PPh_3$[26] (Fig. 2a) allowed for isolation of the **$Mo^nCCH_2Mo^m$** isomers in the absence of ArO•, preventing rapid conversion to the final **$Mo^{IV}CCMo^{IV}$**. Crystals of each isomer were grown from deep green solutions of the coupled product, with the **Mo^V-μ-η^1-η^1-CCH_2Mo^{III}** isomer grown from THF solutions and the **Mo-μ-η^2-η^2-CCH_2Mo** form from benzene or toluene. The core structures are depicted in Fig. 2b, along with key metrical data. Note that the X-ray data acquired for the μ-η^2-η^2 isomer were only sufficient to establish connectivity, so the computed structure for this species is shown in Fig. 2b; for the thermal ellipsoid diagram, see Fig. S8. Despite quite weak C-H bonds, these compounds are relatively kinetically stable and characterized by tolyl methyl peaks at 2.44 and 2.36 ppm in the ^{1}H NMR spectra acquired in d_8-THF or C_7D_8, respectively.

Both **$Mo^nCCH_2Mo^m$** isomers are paramagnetic and we have formally assigned the μ-η^1-η^1 isomer as a Mo^V/Mo^{III} structure based on the short Mo(1)-C(32) distance of 1.800(5) and the long Mo(1)-N(1) distance *trans* to the alkylidene moiety. In comparison, the Mo(2)-C(33) distance of 2.186(6)Å is like that found in **$MoCH_3$** and has a shorter Mo(2)-N(10) bond due to the lower *trans* effect of an alkyl vs. an alkylidyne ligand. Furthermore, an ^{11}B NMR spectrum acquired in d_8-THF exhibits two peaks, consistent with ligands bound to chemically distinct molybdenum centres (Fig. S9), confirming the mixed valence nature of this dinuclear isomer. DFT computations reproduce the metrical attributes of the structure accurately and indicate that a d^3/d^1 configuration is dominant, with the S = 2 and S = 1 spin states very close in energy (Table S5). Assignment of Mo formal oxidation states in the μ-η^2-η^2 isomer, on the other hand, is more ambiguous. DFT computations indicate that S = 1 and S = 0 states are very close in energy. This suggests two of the four d electrons in the dinuclear system are antiferromagnetically coupled across the μ-η^2-η^2 CCH_2 bridge, with the remaining two electrons either spin parallel (S = 1) or spin paired (S = 0, open shell singlet). Metrical data computed for this core indicates more symmetrical bonding within the

Mo-μ-η^2-η^2-CCH_2Mo core, with the Mo-C(63) bonds of ≈ 1.95Å lying between the distances of ≈1.80Å for a Mo≡C triple bond and ≈2.18Å for a Mo-C single bond (Fig. 2b).

Solution magnetic moment measurements and variable temperature NMR experiments indicate that these two **$Mo^nCCH_2Mo^m$** isomers (each of which have two spin states close in energy) are in exchange. Evans method measurements give intermediate μ_{eff} values of 2.90(6) μ_B (THF-d_8) and 2.54(1) μ_B (C_6D_6). Both ^{1}H and ^{11}B NMR spectra in THF-d_8 are highly temperature dependent (Fig. S10-S12). Room temperature spectra are consistent with equilibrating isomers whose fluxionality on the NMR timescale is arrested at low temperatures (-80 deg. C) such that the expected three tolyl methyl signals are observed. The precise speciation and full modelling of this complex system is beyond the scope of this report and more investigation is necessary to fully define the electronic and magnetic properties of the exchanging **$Mo^nCCH_2Mo^m$** isomers.

In any case, the C-H bonds in these **$Mo^nCCH_2Mo^m$** species are sufficiently weakened by CIBW (Fig. 2b) to be rapidly abstracted by ArO• to produce the final ethylenediyl product **$Mo^{IV}CCMo^{IV}$**, which precipitates out of either THF or benzene as a microcrystalline purple powder. It is sparingly soluble in DMF and crystals obtained from this medium confirm its structure (Fig. 2b). The Mo(1)-C(32) and C(32)-C(32') distances of 1.864(3) and 1.335(4)Å, respectively, are consistent with double bonds, and rule out the alternative formulations Mo^{III}-C≡C-Mo^{III} or Mo^{V}≡C-C≡Mo^{V}. The Mo^{IV}=C=C=Mo^{IV} formulation is also consistent with the rigid, crystallographically symmetric arrangement wherein the B_2Pz_4Py ligands are eclipsed across the Mo=C=C=Mo vector (Fig. S13). Although the ^{1}H signals for this compound are somewhat broadened, they all appear in the diamagnetic region of the spectrum, consistent with the fact that an open shell singlet S = 0 state is computed to be the ground state of the molecule by ≈ 23 kcal mol^{-1} over the S = 2 state. Unfortunately, due to the poor solubility of this compound, we have been unable to obtain a ^{13}C NMR spectrum to ascertain the chemical shift for the C_2 bridge.

In summary, we have demonstrated that the (B_2Pz_4Py)Mo^{III} platform is equally effective at inducing C-H bond weakening in a methyl group as it is for activating more protic O-H and N-H bonds. The CIBW of the first C-H bond in **$MoCH_3$** is mainly due to the low voltage (E^0 = 0.08V) observed for the (irreversible) Mo^{III}/Mo^{IV} couple for this complex. However, using the calculated BDFE of 69.0 kcal mol^{-1} (THF solvation) and the C_G value of 59.8 kcal mol^{-1} for THF, measured with the same electrolyte $[NBu_4]^+[PF_6]^-$ employed here,[5, 27] a pK_a of ≈ 5.4 may be estimated for the C-H bond of the putative (unstable) cationic methyl complex **$[MoCH_3]^+$**, which is remarkably low. Given the instability of this cationic methyl species towards homolytic Mo-C bond cleavage, and the likely much higher pK_a of the neutral Mo(III) methyl, the CIBW in complex **$MoCH_3$** enables concerted proton/electron transfer to the ArO• reagent employed, rather than an asynchronous transfer.[28-30] These observations underscore the efficacy of this (**B_2Pz_4Py**)Mo platform for promoting CIBW in a range of E-H bonds.

Author contributions

View Article Online
DOI: 10.1039/D6CC02936A

H. J. D.: Data curation, Investigation, Writing-review and editing; T. R.: Data curation, Investigation; C. C. A.: Investigation, Writing-review and editing; W. Z., C. M.-M.: Data curation (X-ray); A. H.: Methodology; R. A.: Supervision, Resources, Writing-review and editing; L. M.: Conceptualization, Resources, Supervision, Writing-review and editing; W. E. P.: Conceptualization, Data curation, Project administration, Resources, Supervision, Writing-original draft, Writing-review and editing.

Conflicts of interest

There are no conflicts to declare.

Data availability

The data supporting this article have been included as part of the Supplementary Information. Crystallographic data for **$MoCH_3$**, **MoCH**, **Mo^V-μ-η^1-η^1-CCH_2Mo^{III}**, **Mo-μ-η^2-η^2-CCH_2Mo**, and **$Mo^{IV}CCMo^{IV}$** has been deposited at the CCDB under accession codes 2552063-2552067, respectively, and can be obtained free of charge via www.ccdc.cam.ac.uk/data_request/cif.

Acknowledgements

Funding for this work was provided by NSERC of Canada in the form of a Discovery Grant to W.E.P. who also acknowledges the Canada Research Chair secretariat for a Tier I CRC (2020–2027). H.J.D. thanks NSERC for a CGSD scholarship and the University of Calgary for Doctoral Scholarship funding. The computational work was supported by the HPCs CALcul en Midi-Pyrénées (CALMIP-EOS grant 1415); L. M. is a senior member of the Institut Universitaire de France. The authors would like to acknowledge Mr. Jannik Barth for useful discussions.

Notes and references

1. N. G. Boekell and R. A. Flowers, II, *Chem. Rev.*, 2022, **122**, 13447-13477.
2. B. Ruscic, A. F. Wagner, L. B. Harding, R. L. Asher, D. Feller, D. A. Dixon, K. A. Peterson, Y. Song, X. Qian, C.-Y. Ng, J. Liu, W. Chen and D. W. Schwenke, *J. Phys. Chem. A*, 2002, **106**, 2727-2747.
3. J. J. Warren, T. A. Tronic and J. M. Mayer, *Chem. Rev.*, 2010, **110**, 6961-7001.
4. F. G. Bordwell and M. J. Bausch, *J. Am. Chem. Soc.*, 1986, **108**, 1979-1985.
5. R. G. Agarwal, S. C. Coste, B. D. Groff, A. M. Heuer, H. Noh, G. A. Parada, C. F. Wise, E. M. Nichols, J. J. Warren and J. M. Mayer, *Chem. Rev.*, 2022, **122**, 1-49.
6. R. G. Agarwal, C. F. Wise, J. J. Warren and J. M. Mayer, *Chem. Rev.*, 2022, **122**, 1482-1482.
7. M. J. Bezdek, S. Guo and P. J. Chirik, *Science*, 2016, **354**, 730.
8. M. J. Bezdek, I. Pelczer and P. J. Chirik, *Organometallics*, 2020, **39**, 3050-3059.

View Article Online
DOI: 10.1039/D6CC02936A

9. M. J. Bezdek and P. J. Chirik, *Angew. Chem. Int. Ed.*, 2018, **57**, 2224-2228.
10. G. W. Margulieux, M. J. Bezdek, Z. R. Turner and P. J. Chirik, *J. Am. Chem. Soc.*, 2017, **139**, 6110-6113.
11. D. M. Spasyuk, S. H. Carpenter, C. E. Kefalidis, W. E. Piers, M. L. Neidig and L. Maron, *Chem. Sci.*, 2016, **7**, 5939-5944.
12. C. C. Almquist, N. Removski, T. Rajeshkumar, B. S. Gelfand, L. Maron and W. E. Piers, *Angew. Chem. Int. Ed.*, 2022, **61**, e202203576.
13. E. Khaskin, Y. Diskin-Posner, L. Weiner, G. Leitus and D. Milstein, *Chem. Comm.*, 2013, **49**, 2771-2773.
14. M. W. Drover, D. J. Schild, P. H. Oyala and J. C. Peters, *Angew. Chem. Int. Ed.*, 2019, **58**, 15504-15511.
15. M. J. Chalkley, P. H. Oyala and J. C. Peters, *J. Am. Chem. Soc.*, 2019, **141**, 4721-4729.
16. A. D. Chivington, S. Squire, N. Yamamoto, M. Pink, M. D. Griffith, J. Fletcher, Y. Gao, J. M. Zadrozny and J. M. Smith, *Inorg. Chem.*, 2024, **63**, 10221-10229.
17. L. N. Grant, S. Ahn, B. C. Manor, M.-H. Baik and D. J. Mindiola, *Chem. Comm.*, 2017, **53**, 3415-3417.
18. S. Senthil, D. Fehn, M. R. Gau, A. M. Bacon, P. J. Carroll, K. Meyer and D. J. Mindiola, *J. Am. Chem. Soc.*, 2024, **146**, 15666-15671.
19. H. D. A. C. Jayaweera, C. C. Almquist, T. Rajeshkumar, W. Zhou, L. Maron and W. E. Piers, *Inorg. Chem.*, 2025, **64**, 1860-1874.
20. C. C. Almquist, T. Rajeshkumar, H. D. A. C. Jayaweera, N. Removski, W. Zhou, B. S. Gelfand, L. Maron and W. E. Piers, *Chem. Sci.*, 2024, **15**, 5152-5162.
21. C. C. Almquist, T. Rajeshkumar, W. Zhou, L. Maron and W. E. Piers, *J. Am. Chem. Soc.*, 2025, **147**, 40374-40388.
22. N. Elgrishi, K. J. Rountree, B. D. McCarthy, E. S. Rountree, T. T. Eisenhart and J. L. Dempsey, *J. Chem. Ed.*, 2018, **95**, 197-206.
23. T. Daeneke, A. J. Mozer, T.-H. Kwon, N. W. Duffy, A. B. Holmes, U. Bach and L. Spiccia, *Energy Environ. Sci.*, 2012, **5**, 7090-7090.
24. G. R. Fulmer, A. J. M. Miller, N. H. Sherden, H. E. Gottlieb, A. Nudelman, B. M. Stoltz, J. E. Bercaw and K. I. Goldberg, *Organometallics*, 2010, **29**, 2176-2179.
25. G. M. Jamison, A. E. Bruce, P. S. White and J. L. Templeton, *J. Am. Chem. Soc.*, 1991, **113**, 5057-5059.
26. W. J. Transue, J. Yang, M. Nava, I. V. Sergeyev, T. J. Barnum, M. C. McCarthy and C. C. Cummins, *J. Am. Chem. Soc.*, 2018, **140**, 17985-17991.
27. C. F. Wise, R. G. Agarwal and J. M. Mayer, *J. Am. Chem. Soc.*, 2020, **142**, 10681-10691.
28. D. Bím, M. Maldonado-Domínguez, L. Rulíšek and M. Srnec, *Proc. Natl. Acad. Sci.*, 2018, **115**, E10287-E10294.
29. M. K. Goetz and J. S. Anderson, *J. Am. Chem. Soc.*, 2019, **141**, 4051-4062.
30. M. K. Goetz and J. S. Anderson, *J. Am. Chem. Soc.*, 2020, **142**, 5439-5441.

View Article Online
DOI: 10.1039/D6CC02936A

Data availability

The data supporting this article have been included as part of the Supplementary Information. Crystallographic data for **$MoCH_3$**, **MoCH**, **Mo^{V}-μ-η^1-η^1-CCH_2Mo^{III}**, **Mo-μ-η^2-η^2-CCH_2Mo**, and **$Mo^{IV}CCMo^{IV}$** has been deposited at the CCDB under accession codes 2552063-2552067, respectively, and can be obtained free of charge via www.ccdc.cam.ac.uk/data_request/cif.